

1 The localization of chitin synthase mediates the patterned deposition of chitin in developing *Drosophila*
2 bristles.

3 Paul N. Adler

4 Biology Department

5 Cell Biology Department

6 University of Virginia

7 Charlottesville, VA 22904

8

9

10

11

12

13

14

15

16

17

18

19

20

21

22

23

24

25

26

27 **Abstract**

28

29 The insect exoskeleton is a complex structure that is a key for the life style of this very successful group
30 of animals. It contains proteins, lipids and the N-acetyl glucosamine polymer chitin. Chitin is
31 synthesized by the enzyme chitin synthase. In most body regions, chitin fibrils are found in a stack of
32 parallel arrays that can be detected by transmission electron microscopy. Each array is rotated with
33 respect to the layers above and below. In sensory bristles, chitin primarily accumulates in bands parallel
34 to the proximal/distal axis of the bristle. These bands are visible by confocal microscopy providing
35 experimental advantages. We have used this cell type and an edited chitin synthase gene to establish
36 that the bands of chitin are closely associated with stripes of chitin synthase, arguing the localization of
37 chitin synthase plays an important role in mediating the patterned deposition of chitin. This is
38 reminiscent of what has been seen for chitin and chitin synthase in fungi and between cellulose and
39 cellulose synthase in plants. Several genes are known to be essential for proper chitin deposition. We
40 found one of these, *Rab11* is required for the insertion of chitin synthase into the plasma membrane
41 and a second, *duskylike* is required for plasma membrane chitin synthase to localize properly into
42 stripes. We also established that the actin cytoskeleton is required for the proper localization of chitin
43 synthase and chitin in developing sensory bristles.

44

45

46

47

48

49

50

51

52

53

54

55

56

57

58 Introduction

59 Chitin is an abundant and widespread extracellular polymer found in many types of eukaryotic
60 organisms from fungi to vertebrates. It is synthesized by the multi-pass transmembrane enzyme Chitin
61 Synthase (CS). This enzyme has principally been studied in fungi and insects, where chitin plays
62 important structural roles. In fungi, chitin is a constituent of the cell wall and the number of CS genes is
63 quite variable (Merzendorfer, 2011). For example, *S. cerevisiae* has 3 CS genes (Gohlke et al., 2017)
64 while *Aspergillus fumigatus* has 8 (Muszkieta et al., 2014). Chitin in fungal cell walls is not uniformly
65 distributed and in these systems, different CS's appear to have different subcellular localizations and to
66 mediate chitin synthesis in different parts of the cell wall including the bud ring in budding yeast (Cabib
67 and Bowers, 1971; Foltman et al., 2018). In insects, chitin is a major component of the cuticular
68 exoskeleton, the apical surface of trachea and the peritrophic membrane that lines the gut
69 (Merzendorfer, 2011). In the cuticle, it is typically in parallel arrays while in the peritrophic membrane it
70 is a fibrous mesh. There are two CS genes in insects, one functions in the formation of the cuticular
71 exoskeleton and tracheal lining and the other synthesizes the chitin found in the peritrophic membrane
72 (Merzendorfer, 2011). In *Drosophila* the *kkv* gene encodes the CS enzyme required for the synthesis of
73 cuticle chitin (Moussian et al., 2005; Ostrowski et al., 2002).

74 The most conserved region in all chitin synthases is the catalytic domain (con1) (Dorfmueller et al., 2014;
75 Nagahashi et al., 1995; Yabe et al., 1998) and this region is essential and sufficient for chitobiose
76 synthesis by SC-CHS2. A second conserved region (con2) is essential for the synthesis of long chito-
77 oligosaccharides, and seems likely to be essential for the translocation of growing chitin chains
78 (Dorfmueller et al., 2014; Yabe et al., 1998). Both of these regions are thought to be cytoplasmic in
79 yeast CHS2, although there is evidence for two transmembrane domains separating the catalytic site
80 from at least the c terminal most part of Con2 (Gohlke et al., 2017). The number of inferred
81 transmembrane domains varies from ~5 to 18 with fungal CS proteins generally predicted to contain
82 many fewer putative transmembrane domains than insect CS proteins (Gohlke et al., 2017;
83 Merzendorfer, 2011) (Merzendorfer and Zimoch, 2003). In the case of fungal chitin synthases direct
84 experimental data established that the computer programs for predicting transmembrane domains are
85 useful but not able to predict accurately membrane protein topology (Gohlke et al., 2017). We report
86 here experimental evidence that the amino terminus of *Drosophila* Kkv is in the cytoplasm and the
87 carboxy terminus in the extracellular space.

88 The arrangement of chitin in insect cuticle may differ in different structures. Over most of the cuticle it
89 is in layers of parallel arrays of chitin fibrils with each layer rotated with respect to its neighbors above
90 and below (Bouligand, 1972; Moussian, 2013; Moussian et al., 2006a). As assayed by confocal
91 microscopy, in the cuticle that covers the shaft of sensory bristles chitin is most abundant in bands that
92 run parallel to the proximal-distal axis of the bristle (Nagaraj and Adler, 2012). In transmission electron
93 micrographs, we did not see evidence for the presence of chitin layers in bristles or in hairs (trichomes).
94 Whether this represents a true difference or is a consequence of a higher density of cuticle proteins
95 masking the layers remains uncertain. In this paper, we make use of the bristle shaft as a model cell
96 type to study patterned chitin deposition in insects. The large size of these polypoid cells makes them
97 favorable for this purpose.

98 Chitin fibrils are insoluble at physiological pH (Elieh-Ali-Komi and Hamblin, 2016), which restricts models
99 for patterned chitin deposition (Fig 1A). One possibility is that in insects as in fungi CS is localized in a
100 patterned way to specific membrane domains and chitin deposition is directly patterned by this. In
101 insect epidermal cells rows of elevated membrane called undulae have been proposed to be the site of
102 chitin deposition (Moussian et al., 2007) (Moussian et al., 2006a). The tips of the undulae are associated
103 with secreted extracellular matrix (Moussian et al., 2006a) (Adler, 2017) but it is not clear if this material
104 is composed of chitin, cuticle proteins, other extracellular proteins/carbohydrate or more than one (or
105 all) of these. Interestingly, prominent undulae are not seen during the deposition of some chitin
106 containing cuticle, for example the cuticle that covers wing hairs or bristles (Adler, 2017; Sobala and
107 Adler, 2016). Thus, it seems unlikely that undulae per se are essential for chitin or cuticle deposition.
108 An alternative model is that the synthesis of chitin is not patterned but that chitin binding proteins bind
109 to chitin fibrils as they are extruded through the membrane and serve as carriers to mediate the
110 movement of the chitin to the correct place in the developing cuticle. There are a large number of
111 proteins encoded by insect genomes that contain a chitin binding domain and could be part of such a
112 system (Karouzou et al., 2007; Willis, 2010). In such a model, it seems likely that one or more
113 unidentified proteins are first deposited in a patterned way and they interact with the chitin binding
114 protein-chitin complex to guide the location for chitin fibril deposition. A third model is that CS
115 containing exosomes/chitosomes are secreted and these are guided to the correct location for by
116 interactions between exosome membrane proteins and one or more cuticle components. There are
117 suggestions in support of this sort of model in the literature but evidence for exosomes has not been
118 reported in transmission EM studies on cuticle deposition in *Drosophila* (e.g. (Sobala and Adler, 2016)).

119 We used the accumulation of chitin bands in sensory bristle cuticle (Nagaraj and Adler, 2012) to
120 examine the relationship between the localization of Chitin Synthase (Kkv) to the patterned
121 accumulation of chitin. We find Kkv is closely associated with these chitin bands during cuticle
122 deposition. Notably, this is true even when both patterns are highly abnormal. The accumulation of Kkv
123 is not smooth like the chitin bands but is punctate. To clarify the text we use stripes to describe the
124 accumulation of Kkv and bands to describe chitin. We previously identified several genes whose
125 function was essential for the accumulation of bristle chitin in parallel bands (Nagaraj and Adler, 2012).
126 Knocking down the function of two of these genes resulted in a failure of the accumulation of Kkv in
127 stripes. These observations link the patterning of extracellular chitin to the patterning of Kkv
128 localization in the apical plasma membrane of epithelial cells and begin the identification of genes that
129 mediate both the insertion of Kkv into the plasma membrane and the patterned organization of Kkv in
130 stripes along the proximal distal axis of the bristle.

131

132 **Results**

133 **Generation and characterization of transgenes and edited genes that encode tagged Kkv.**

134 As a first step in examining the role of CS localization in the patterning of chitin deposition we generated
135 a series of new genetic reagents consisting of 4 different *UAS-kkv* transgenes and two edits of the
136 endogenous *kkv* gene (Fig 1BC) (see Methods for details).

137 In one of the *UAS* transgenes the *kkv* open reading frame was tagged on the C terminus by the bright
138 mNeonGreen (NG) fluorescent protein (Shaner et al., 2013) (*UAS-kkv::NG*). In a second it was tagged by
139 the ollas epitope tag (Park et al., 2008) and his₆ (*UAS-kkv-OH*). Overexpression of these transgenes
140 resulted in mild and limited gain of function phenotypes (see Supplementary Text File 1 and Fig S1). We
141 also examined a variant of the NG tagged protein that contained the amino acid change found in the
142 amorphous *kkv-1* allele (R896K) (Moussian et al., 2005). In the fourth, multiple changes converted the
143 catalytic domain to change convert it to the equivalent mosquito sequence.

144 We used CRISPR/Cas9 and Homology Dependent Repair (HDR) to edit the endogenous *kkv* gene to add
145 two different C terminal tails (see Methods for details). In one we added the mNeonGreen fluorescent
146 protein (NG) (Shaner et al., 2013) while in the second we added *smFP-HA* (Viswanathan et al., 2015) (Fig
147 1BC), which is a variant of super folder GFP with multiple HA tags inserted into loops of GFP. Both
148 *kkv::NG* and *kkv::smFP-HA* were homozygous viable and showed no mutant phenotypes under a stereo
149 microscope. Homozygous *kkv::NG* fly cuticle appeared normal when examined by compound light
150 microscopy or scanning electron microscopy (Fig 2EF, S2CD – compare to EF). This was also true for
151 *kkv::NG/DF* and *kkv::NG/kkv¹*. The data establish the edited gene and protein are close to if not
152 functionally equivalent to wild type. Homozygous *kkv::smFP-HA* flies displayed a phenotype of thin and
153 bent hairs wing hairs (Figs 2EF, S2A). The phenotype appeared slightly stronger in *kkv::smFP-HA/Df* flies
154 but we did not attempt to quantify this (Fig S2AB). In *ap-Gal4; UAS-kkv::NG kkv::smFP-HA/kkv::smGFP-*
155 *HA* and *ap-Gal4; UAS-kkv::NG kkv::smFP-HA/Df(3R)ED5156* flies the wing hair phenotype was rescued in
156 the dorsal wing cells where *ap* drives expression of *kkv::NG* but not in the ventral wing cells that served
157 as an internal control (Fig 2GH). Similar results were obtained when *UAS-kkv-OH* was substituted for
158 *UAS-kkv::NG*. We examined pupae that expressed *Kkv::NG* and *Kkv::smFP-HA* by in vivo confocal
159 imaging. The level of fluorescence was much higher for *Kkv::NG* (we estimate it as being ~15X brighter
160 (see Methods and Fig S3)) and hence we used it for all of the protein localization experiments described
161 below. These data are consistent with *kkv::smFP-HA* being a viable hypomorphic allele of *kkv* where a
162 lower than normal level of protein accumulates. The hair phenotype is likely due to this structure
163 requiring a higher level of chitin for normal morphogenesis. Consistent with this hypothesis wing
164 trichomes are also the most sensitive cuticular structure to knocking down *kkv* expression using RNAi
165 (pna, unpublished).

166

167 **Subcellular Localization of Kkv**

168 *Kkv::NG* localized to the apical surface of the large polytene salivary gland cells in *ptc>kkv::NG* larvae
169 (Fig S4I). In *ptc>kkv::NG* wing discs we observed the expected stripe of expression (Fig S5A) in the
170 middle of the wing. We saw no evidence for the secretion of *Kkv::NG* in these experiments. The stripe
171 was obvious in living wing discs and in fixed wing discs stained with anti-NG antibodies, establishing the

172 specificity of the antibodies. A similar specificity was observed for a rabbit polyclonal antibody (anti-
173 Kkv-M) made against a region from the central part of the Kkv protein (aa1097-1246) and an anti-ollas
174 monoclonal antibody. As expected (Maue et al., 2009; Moussian et al., 2015; Zimoch and
175 Merzendorfer, 2002) Kkv::NG was preferentially localized apically in wing disc cells (Fig S5B, arrow). In
176 *ap>kkv::NG* pupal wings Kkv::NG was localized external to the actin filaments found in the center of
177 growing hairs (Fig 3G-L) (Adler et al., 2013; Turner and Adler, 1998; Wong and Adler, 1993). This close
178 localization is reminiscent of apical F-actin and chitin in wing hairs (Adler et al., 2013) and in late stages
179 of trachea development in *Drosophila* embryos (Ozturk-Colak et al., 2016).

180 The use of the Neon Green (and Ollas-His₆) tag to localize Kkv requires that the tag remains associated
181 with the enzyme. Since chitin synthases are often cleaved and this has been linked to enzyme activation
182 (Broehan et al., 2007; Merzendorfer and Zimoch, 2003) (Zhang and Zhu, 2013) this is a concern (we have
183 also seen evidence for cleavage of Kkv on Western blots - pna, preliminary results). To test if the tags
184 remained associated with the enzyme we stained pupae with both a commercially available anti-NG
185 monoclonal and our anti-Kkv-M rabbit polyclonal antibody. We observed a clear co-localization in
186 stripes of puncta along the proximal distal axis in bristles (Fig 4 DEF). This established that the neon
187 green tag from the fusion protein is an accurate reporter for the Kkv protein. We obtained similar results
188 using anti-Ollas and anti-Kkv antibodies (Fig 4 GHI).

189 **Localization of Kkv encoded by the edited endogenous gene:**

190 We first examined the accumulation of Kkv::NG in pupal wings as this tissue is best characterized for the
191 timing of cuticle deposition and gene expression (Adler et al., 2013; Sobala and Adler, 2016). Previously
192 we found that we could first detect chitin in developing hairs wing hairs around 42 hr after white
193 prepupae (awp) (Adler et al., 2013). We observed Kkv::NG in developing hairs in living pupal wings at
194 42, 49 and 58 hrs awp (after white pupae) (Fig 3C). The level of fluorescence was lower in 42 hr hairs
195 than in 49 hr hairs. We could also detect Kkv::NG fluorescence in the apical surface of wing cells at
196 these times with higher levels at cell boundaries. This was a bit surprising since the procuticle
197 deposition starts later (~ 56-58 hr awp) in the wing blade (Adler et al., 2013; Sobala and Adler, 2016). In
198 digitally enhanced images we also observed evidence for Kkv::NG in 38 hr awp wings in the proximal
199 part of the hair (Fig 3B). In older wings (e.g. 76 hr) during the middle of procuticle deposition the apical
200 membrane fluorescence was stronger than at earlier times and we could see the pedestals that the hairs
201 are found on at late stages (Fig 3F) (Mitchell et al., 1990; Sobala and Adler, 2016).

202 We next examined Kkv::NG in thoracic bristles by in vivo imaging from ~40-80 hr awp. Previously we
203 found that chitin accumulated in bands along the proximal distal axis of thoracic bristles starting around
204 42 hr awp (Nagaraj and Adler, 2012). The level of Kkv::NG fluorescence in younger than 50hr awp
205 bristles was lower than in older bristles. (Fig S6). At both early and later stages, Kkv::NG fluorescence
206 had a punctate appearance within an overall pattern of stripes along the proximal distal axis of the
207 bristle (Figs 4A-C, 5J, S5E, S6). As development proceeded, the stripes became more complete although
208 they never reached the completeness and smoothness seen with chitin bands. In older animals (>70
209 hrs) the pattern became somewhat less distinct with more inter-stripe fluorescence (Fig S6). When we
210 examined orthogonal views of bristle image stacks the stripes of Kkv were obvious (Fig 6A). Unless

211 stated otherwise we examined bristles from 50-65 hr old animals as these showed the most dramatic
212 “stripe pattern”. Control experiments with Oregon-R pupae established that the florescence we were
213 observing was due to the edited *kkv* gene and not to autofluorescence (Fig S5C-F). A similar, albeit
214 perhaps a bit less precise stripe pattern was seen in developing *neur-Gal4, UAS-Kkv::NG* bristles.

215 To investigate the localization of chitin and CS we carried out experiments where we localized both
216 *Kkv::NG* and our chitin reporter (Cht-Vis) in bristles in living pupae (Sobala et al., 2015). The bands of
217 ChtVis differed from those of *Kkv::NG* by being smooth rather than punctate (Fig 4C-C’). However, the
218 two patterns were largely co-aligned in stripes. In cross section the ChtVis signal was usually exterior to
219 the *Kkv-NG* signal as expected for chitin being secreted and CS being in the plasma membrane (Fig 6B,
220 arrows). The stripe of *Kkv::NG* was often also offset a bit from the ChtVis signal, which could be a
221 consequence of ChtVis reporting on chitin (an accumulated product) while the *Kkv::NG* signal represent
222 protein at a particular instance in time. The different cellular location (plasma membrane vs
223 extracellular) and geometry likely contributes to this (Fig S7).

224

225 **The actin cytoskeleton influences the accumulation of Kkv**

226 We also explored the relationship between *Kkv::NG* accumulation and the large bundles of cross-linked
227 F-actin found in bristles (Tilney et al., 1995). These experiments were complicated by the breakdown of
228 the actin bundles, which starts around 43 hr (Guild et al., 2002), and our inability to reliably
229 immunostain bristles older than about 48 hr awp. In our best experiments we examined pupae that
230 were 48hr or younger. An additional complication is geometric and due to *Kkv* being in the plasma
231 membrane (and the NG in *Kkv::NG* being extracellular as described below) while the F-actin extends
232 some distance into the cytoplasm (Tilney et al., 1995) (Fig S7). Using an F-actin reporter (Lifeact-Ruby -
233 (Hatan et al., 2011; Riedl et al., 2008) we observed a close connection between the localization of
234 *Kkv::NG* and the large bundles of F-actin in *neur>lifeact-Ruby; kkv::NG* pupae. The results varied from
235 the two appearing to co-localize to their being slightly offset (Fig 5H-J, H’-J’) consistent with the
236 geometry considerations (Fig S7).

237 The large bundles of highly cross-linked actin filaments support the shape and growth of developing
238 bristles and in their absence in *sn³ f³⁶* double mutants the resulting bristles are bent, curved, split,
239 shorter and stand more upright than normal (Guild et al., 2002; Tilney et al., 2004; Tilney et al., 1995).
240 In separate experiments, we observed an abnormal distribution of chitin and *Kkv::NG* in living *sn³ f³⁶*
241 double mutants. The robust parallel array of chitin bands and *Kkv::NG* stripes were severely disrupted
242 (Fig 5AB). *Kkv::NG* was primarily in the plasma membrane and the chitin appeared to be extracellular so
243 the bundles of F-actin do not appear to be required for the localization of either. To determine the
244 relationship between the abnormal stripes of *Kkv::NG* and chitin we examined the distribution of both in
245 the same living bristle. We found substantial co-localization of chitin and *Kkv::NG* conserved in these
246 highly abnormal bristles (Fig 5CDE).

247 **Proteins required for the proper localization of Kkv.**

248 We previously established that Rab11 and exocyst function is required for the deposition of cuticle and
249 the bands of chitin in bristles (Nagaraj and Adler, 2012). Affected bristles become unstable and collapse
250 after the highly cross-linked F-actin bundles in developing bristles begin to depolymerize (Guild et al.,
251 2002; Nagaraj and Adler, 2012). To determine if this was associated with improperly localized CS we
252 examined Kkv::NG in thoracic bristles of living *neur-Gal4 Gal80-ts/Rab11 RNAi; kvv-NG/kkv-NG* pupae
253 shifted to 29.5°C at wpp (white prepupae). These animals developed the extreme stub macrocheatae
254 phenotype (Fig 5G, arrow) described previously (Nagaraj and Adler, 2012). The morphology of the
255 developing bristles depended on pupal age. In the youngest animals examined, the bristles showed the
256 blebbing characteristic of the early stages of the collapse program (Nagaraj and Adler, 2012). In older
257 animals the collapsed stub bristle morphology was seen (Fig 5G, arrow). The stripes of Kkv::NG were
258 lost and in Z sections we found that the protein was cytoplasmic (Fig 6C). Thus, Rab11 function is
259 required for the insertion of Kkv into the plasma membrane and hence the loss of chitin bands in the
260 mutant (Nagaraj and Adler, 2012).

261 The Zona Pellucida domain Dusky-Like (Dyl) protein acts as a Rab-11 effector for chitin deposition in
262 bristles (Nagaraj and Adler, 2012). We examined living *UAS-dyl-RNAi/+; neur-Gal4 kvv::NG/kkv::NG*
263 pupae and observed the bristle blebbing phenotype was associated with the loss of the robust striping
264 pattern of Kkv::NG accumulation (Fig 5F, arrow). Kkv::NG in such bristles was primarily spread around
265 the plasma membrane (Fig 6D). The distribution was not uniform but was far from the nicely spaced
266 stripes seen in wild type. The data indicate that Dyl is required for the localization of Kkv::NG in stripes
267 but not for its insertion into the plasma membrane. The difference in Kkv::NG localization between the
268 Rab11 and Dyl knockdowns suggests that these two genes and proteins mediate different steps in the
269 localization of Kkv.

270 We also simultaneously localized Kkv-NG and Dyl in bristles by immunostaining. The stripes of Kkv::NG
271 and Dyl were interdigitated but did not appear to touch (Fig 5KLM, arrow). We further established that
272 the large actin bundles are essential for the accumulation of Dyl in stripes in bristles (Fig S8AB).

273

274 **Localization of an inactive mutant Kkv**

275 We next addressed whether the catalytic activity of Kkv might impact its subcellular localization by
276 placing a R896K mutation into *UAS-kkv::NG*. This missense mutation is the cause of the amorphic *kkv*¹
277 allele and is in an invariant site that is part of the enzyme's active site (Dorfmueller et al., 2014;
278 Merzendorfer, 2006; Moussian et al., 2005; Nagahashi et al., 1995). We first tested if this transgene
279 could rescue the wing hair phenotype seen in *kkv::smFP* flies. The wings of *ap-Gal4/+; UAS-kkv-*
280 *R896K::NG kvv::smFP/kkv::smFP* flies showed no evidence of rescue of the *kkv::smFP* hair phenotype
281 (Fig 2IJ). The failure of this transgene, which encodes a protein that very likely has little or no catalytic
282 activity, provides support for the validity of the *kkv::smFP* rescue assay.

283 We observed a failure of the normal apical localization of Kkv-R896K::NG in salivary gland cells (compare
284 Fig S4I and J). At higher magnification, we observed Kkv::NG accumulated in vesicles that contained
285 bright puncta (Fig S4I', arrow). In contrast the mutant protein accumulated either between vesicles or in

286 abnormally shaped vesicles (Fig S4 J'). Kkv-R896K::NG also failed to accumulate in pupal wing hairs (Fig
287 S4A-D) and it did not accumulate in stripes in bristles (Fig S4E-H). As a control we immunostained pupal
288 wings and bristles that expressed Kkv-R896K::NG using both the anti-NG and anti-Kkv-M antibodies, and
289 observed extensive co-localization (Fig S9S-F). Hence, the mislocalization was not due to cleavage of the
290 NG reporter from the mutant protein.

291

292 **A Kkv with a catalytic domain mutated to a mosquito catalytic domain is functional.**

293 We next attempted a more ambitious test of the *kkv-smFP* rescue assay using a UAS transgene where
294 the con1 domain of *kkv* was replaced by the equivalent region of a mosquito chitin synthase (*UAS-kkv-*
295 *mos::NG* – see Fig 1B and Methods for details). We generated *ap-Gal4/+; UAS-kkv-mos::NG*
296 *kkv::smFP/kkv::smFP* flies and found that the mutant wing hair phenotype of *kkv::smFP* to be fully
297 rescued in the dorsal but not ventral wing surface hairs (Fig 2KL) indicating that this “hybrid” protein is
298 active.

299

300 **Topology of Kkv**

301 Reagents we generated for other reasons provided us with tools we could use to probe the topology of
302 Kkv. Using a collection of programs to predict the location of transmembrane domains led us to a
303 consensus of 14 predicted transmembrane domains (Fig 7B and Methods). We found both anti-NG and
304 anti-Ollas antibodies stained wing discs expressing the relevant transgene in the absence of
305 permeabilization indicating that the C terminus is exposed to the extracellular space (Fig 7A). All of the
306 topology programs predicted this. In contrast when we used an anti-Kkv polyclonal antibody (anti-Kkv-
307 M) raised against aa 1097-1246 we did not see any staining in the absence of Triton X-100
308 permeabilization (Fig 7A), arguing this region is intracellular. This disagrees with the consensus
309 prediction. Similar results were obtained when we used antibodies directed against aa 53-66 and also
310 antibodies directed against aa 530-541 – a region located not far from the catalytic domain (Fig 7AB). It
311 is worth noting that no programs predicted a transmembrane domain in the region encompassing aa 1-
312 53, which when combined with our data suggests that the amino terminus of Kkv is located in the
313 cytoplasm.

314

315 **Discussion:**

316 **The patterning of Chitin deposition in bristles is linked to the localization of Kkv.**

317 Our observations establish that the localization of chitin deposition is closely linked to the localization of
318 Kkv (Chitin synthase) in bristles. The most compelling data being that chitin and Kkv remain largely
319 colocalized even when the distribution of both is highly abnormal. A limitation of our observations is
320 that they focused on the bands of chitin seen in developing sensory bristles. The cuticle that covers the

321 sensory bristles differs in two ways from the cuticle that covers much of the fly's body. First, we have
322 not detected the layering of chitin in TEM studies of bristles although this could simply be due to a
323 higher concentration other components in bristle procuticle interfering with our ability to detect the
324 layering. A second difference is that the prominent undulae seen in most cells synthesizing cuticle were
325 not detected in bristle forming cells (Adler, 2017). Further studies are needed to determine if the
326 linkage between chitin and chitin synthase is a general result for arthropod epithelial cells. The close
327 connection between CS and chitin is similar to that seen in yeast and fungi (Leal-Morales et al., 1994)
328 (Chuang and Schekman, 1996) (Santos and Snyder, 1997) (Kozubowski et al., 2003) (Latge et al., 2005)
329 and is reminiscent of the connection between cellulose and cellulose synthase in plants (Polko and
330 Kieber, 2019).

331
332 The localization of Kkv in bristles requires both the intracellular transport of the protein into the plasma
333 membrane and its restriction to stripes. We previously identified *Rab11* and *dyl* as being essential for
334 the normal deposition of chitin in bands in bristles (Nagaraj and Adler, 2012). We established here that
335 in the absence of *Rab11* function Kkv::NG failed to localize to the plasma membrane. In contrast, in the
336 absence of *dyl* function Kkv::NG localized to the plasma membrane but not preferentially accumulate
337 into the appropriate stripes. These results argue that these two genes mediate different steps essential
338 for the localization of Chitin Synthase. Rab11 is also required for the insertion of Dyl into the plasma
339 membrane of developing bristles (Nagaraj and Adler, 2012) and we suspect it has a general role for
340 insertion of proteins into the shaft plasma membrane. The role of *dyl* is of particular interest. Dyl is a ZP
341 (zona pellucida) domain protein and like other ZP domain proteins it can polymerize (Adler et al., 2013;
342 Jovine et al., 2005; Jovine et al., 2002) and it is thought that this allows it to organize the apical
343 extracellular matrix (Chanut-Delalande et al., 2012; Fernandes et al., 2010). The expression of *dyl* is
344 almost entirely restricted to the period of envelop deposition (Sobala and Adler, 2016) and it
345 accumulates in bands along the proximal distal axis of developing bristles (Nagaraj and Adler, 2012).
346 Hence, it localizes in a way that is appropriate for instructing the later accumulation of Kkv in stripes. I
347 observed that the stripes of Kkv::NG and Dyl were interdigitated and did not overlap. I suggest that that
348 Dyl functions as a negative factor to inhibit the accumulation of Kkv::NG from regions of the bristle
349 plasma membrane, but likely does so indirectly as there appears to be space between the interdigitated
350 bands. Future studies will be needed to elucidate the mechanisms involved here (e.g. local Dyl could
351 recruit a factor that removes Kkv::NG from nearby regions of the membrane). In addition to Rab11 and
352 Dyl we also established that the large bundles of cross linked F-actin in bristles were also required for
353 the normal deposition of chitin bands. The localization of both Dyl and Kkv::NG were altered in
354 developing *snf* bristles. The mislocalization of Dyl provides a mechanism for the mislocalization of
355 Kkv::NG and the subsequent abnormal chitin deposition in *dyl* mutant bristles. A number of other genes
356 have been identified that are required for normal chitin deposition or where a loss of function leads to a
357 *kkv* like wing hair phenotype (Adler et al., 2013; Chaudhari et al., 2011; Moussian et al., 2015; Moussian
358 et al., 2006b). It will be interesting to determine which, if any of these also mediate Kkv localization.

359

360 It is possible that Kkv is actively cycled from the plasma membrane to cytoplasmic
361 endosomes/chitosomes and then back to the plasma membrane. There is strong evidence for the

362 recycling of chitin synthase in yeast (Hernandez-Gonzalez et al., 2018; Knafler et al., 2019; Sacristan et al.,
363 2013) and Rab11 is a well-established marker for late endosomes (Calero-Cuenca and Sotillos, 2018)
364 (Welz et al., 2014) and the recycling of membrane proteins. In such a model the failure of Kkv::NG
365 localization in Rab11 deficient bristles could be due to a defect in recycling and not in the original
366 localization. This might also explain the failure of the presumptive catalytic defective Kkv-R896K mutant
367 protein to localize to the plasma membrane. It is possible that the inactive protein is more rapidly
368 removed from the membrane and that it is preferentially not recycled back to the plasma membrane or
369 recycled more slowly. This could be a quality control mechanism in the formation of insect cuticle.

370

371 ***kkv::smGFP* is useful as a system for structure function studies on CS.**

372 The importance of chitin synthase function for insects is demonstrated by the lethality associated even
373 with moderately small clones of *kkv* mutant cells (Ren et al., 2005) (Adler et al., 2013) and knocking
374 down *kkv* function for a restricted period of time in a limited set of epidermal cells (pna - unpublished).
375 The edited *kkv::smFP* allele is the only homozygous viable hypomorphic allele of *kkv* that we are aware of.
376 As we demonstrated the rescue of the wing hair phenotype of *kkv::smFP* is an easy assay for testing the
377 functionality of mutant Kkv proteins. This assay relies on UAS-Gal4 driven expression and this could be
378 misleading as overexpression could prevent distinguishing between mutants with reduced vs completely
379 normal activity. There are however, advantages to this assay compared to editing the endogenous
380 gene. It is important to consider that while CRISPR/Cas9 mediated editing is not difficult it still involves
381 more time and labor than UAS transgenesis and mutations identified as interesting by the UAS-Gal4
382 system can later be assessed using CRISPR/Cas9 to test for reduced but still significant chitin synthase
383 activity. Further, chitin synthases are known to function as multimers (Merzendorfer, 2011) (Gohlke et
384 al., 2017) and some mutations might be dominant negatives. These could be identified using the UAS-
385 Gal4 system but they would likely fail to be recovered by CRISPR/CAS9 mediated editing (or by classical
386 mutagenesis) as they are likely to be dominant lethals. The UAS/Gal4 system could also be used to
387 identify parts of the Kkv protein that are essential for its localization. The rescue by the Kkv-mos::NG
388 protein indicates that the system should be able to assess at least in part the function of non-Drosophila
389 chitin synthases.

390 It was not surprising that the *kkv R896K* mutant showed no rescue activity as this missense mutation is
391 considered an amorphic allele in Drosophila (Moussian et al., 2005) and a similar substitution in yeast
392 contained only about 1% of wild type activity (Nagahashi et al., 1995). The failure of Kkv R896K to show
393 rescue activity validates the rescue system for structure function studies on the fly CS. It was surprising
394 that this mutant protein did not localize properly. It is possible that the active site missense mutation
395 disrupts both catalytic activity and normal protein folding and the folding defect leads to a failure to
396 traffic the protein to the apical plasma membrane. As noted above it is also possible that the defect is
397 not in the initial trafficking but is due to the inactive protein being removed more quickly. Further
398 studies will be required to distinguish between these hypotheses.

399 The *kkv::NG* and *kkv-smFP* edits were in the same location in the genome so it is likely that the greater
400 activity and fluorescence of the *kkv::NG* edit compared to the *kkv-smFP* edit is not due to differences in
401 transcription. Rather, our data suggests the smFP tagged only accumulates to a much lower level than
402 the NG tagged protein. This could be due to a reduced half-life of the smFP tagged protein or to it
403 folding less efficiently. One possible cause of this is the presence of multiple copies of the HA epitope
404 tag in smFP. A study in yeast reported that a 3XHA tag could cause a dramatic decrease in the
405 accumulation of some of the tagged proteins (Saiz-Baggetto et al., 2017). It is possible that a similar
406 phenomenon can explain our results with *kkv-smFP*.

407 **Kkv is present in the plasma membrane prior to procuticle formation.**

408 Previous studies on the transcriptome of pupal wing cells (Ren et al., 2005; Sobala and Adler, 2016)
409 established that *kkv* RNA was present prior to the start of wing blade procuticle deposition. Part of the
410 reason for this is that wing hair chitin is deposited earlier than wing blade chitin. However, this cannot
411 explain the presence of *kkv* RNA 8 hrs prior to the start of hair morphogenesis and 16 hrs prior to the
412 earliest time we can detect hair chitin (Ren et al., 2005) (Adler et al., 2013). Neither can it explain the
413 presence of Kkv protein in the general apical membrane (i.e. not in the hair) more than 12 hrs prior to
414 blade procuticle deposition. These observations suggest the possibility that Kkv has an earlier function
415 in cuticle formation that is not due directly to chitin synthesis (e.g. a structural role for the protein) or
416 that the synthesis of unstable chitin could be important prior to the time when it begins to accumulate.
417 Both of these hypotheses suggest it might be possible to detect abnormalities at early stages of cuticle
418 formation in *kkv* mutant cells.

419 **Similarities and differences in bristle and tracheal chitin deposition.**

420 Chitin deposition in bristles and the adult cuticle shows both similarities and differences from that
421 described in trachea. In trachea the distribution of chitin changes during development. Starting out as a
422 thick filament that largely fills the lumen it transforms into a thin zig zag shaped filament. The thin
423 filament is eventually lost and during the this period chitin becomes concentrated over the distinctive
424 tracheal taenidial folds (Devine et al., 2005; Ozturk-Colak et al., 2016; Tønning et al., 2005). It is not
425 clear whether there is a complete loss of the chitin fibrils found in the central filament or if there is a
426 reorganization of those fibrils into the taenidial fold chitin. In both tissues the disruption of the actin
427 cytoskeleton results in an abnormal pattern of chitin; however in tracheal development a lack of chitin
428 lead to an abnormal actin cytoskeleton while we did not see that in wing cells that lacked Kkv (Adler et
429 al., 2013). In trachea Kkv puncta were seen more frequently over the taenidial folds than in the inter-
430 fold region (Ozturk-Colak et al., 2016) but the patterning was less distinctive than we have seen in
431 bristles. Some of the differences between these results could be due to the use of UAS-Gal4 to drive the
432 expression of Kkv in trachea as in our hands using UAS-Gal4 to express *kkv* in bristles resulted in a
433 “messier” pattern than was observed using the edited *kkv* gene. This is presumably due to UAS-Gal4
434 leading to overexpression.

435

436 **Methods and Materials**

437 Fly Stocks and Genetics

438 Flies were grown on standard fly food. They were routinely raised at 25°C, but in some experiments,
439 they were raised at 21°C to slow development. In other experiments we used a temperature sensitive
440 Gal80 to limit UAS transgene expression (McGuire et al., 2004). In these experiments, the animals were
441 grown at 21 °C or 18 °C and then at the desired stage transferred to 29.5°C to inactivate the Gal80 and
442 induce the expression of the UAS transgene. The various RNAi inducing transgenes came either from the
443 VDRC (Dietzl et al., 2007) or TRiP collections (Perkins et al., 2015). The VDRC lines were obtained from
444 the VDRC (<http://stockcenter.vdrc.at/control/main>). The TRiP lines were obtained from the
445 Bloomington Drosophila Stock Center (<http://flystocks.bio.indiana.edu/>) (NIH P40OD018537) as were
446 many other lines used in the research (e.g. Gal4 lines, Df stocks, *kkv*¹ carrying stock). Flies that carried a
447 *y w sn³ f³⁶⁰* X chromosome were kindly provided by G. Guild. Other stocks were made by the author in
448 his lab.

449 Constructs for generating transgenic lines.

450 UAS constructs

451 The UAS constructs were in the pUAST-attb vector (Bischof et al., 2007). There are 3 *kkv* mRNA isoforms
452 that encode two distinct *kkv* proteins (Thurmond et al., 2018). All of our experiments and analyses were
453 done with the A isoform unless stated otherwise. The C protein isoform is identical to the A isoform and
454 both contain 1615 aa. The D isoform also contains 1615 aa but it differs from the other two proteins by
455 14 aa due to its mRNA containing an alternative coding exon. The 14 amino acids are found in the
456 region bounded by aa 1277 and 1322 of the A isoform. A comparison of the sequence of the genomic
457 *kkv* gene and the longest *kkv* cDNA (RE32455) from the Drosophila genome project revealed two
458 putative single base pair deletions in RE32455. A comparison of conceptual translation with those of
459 other chitin synthases showed that the genomic sequence was correct. The two single base pair
460 deletions were repaired by site directed mutagenesis to correspond to the genomic sequence. The
461 cDNA was amplified and fused to the coding region for Neon Green *kkv* by Gibson assembly (NEB-
462 E2611). This fusion gene was inserted into pUAST-attb using added Xho1 and Xba1 sites present in
463 pUAST-attb and added to *kkv::NG* during construction using PCR and oligos containing the sites. This
464 plasmid is referred to as *UAS-kkv::NG* (Addgene-138953). A similar strategy was used for the construct
465 where the Neon Green tag was replaced by the *ollas*-his₆ (OH) tag (Addgene - 138956). The nucleic acid
466 sequences are provided in supplementary files S1 and S2 and the sequences of the tagged Kkv proteins
467 are provided in files S3 and S4. The *UAS-kkv-R896K::NG* plasmid (Addgene – 138957) used for
468 transgenesis was made by site directed mutagenesis of *UAS-kkv::NG*. Although an R to K substitution is
469 generally considered a conservative substitution R896 is conserved in all chitin synthases and is thought
470 to be at the catalytic site. In addition, the R to K change is found in the amorphic *kkv*¹ mutation in
471 Drosophila (Moussian et al., 2005). The same R to K mutation in yeast Chs2 resulted in a reduction to ~
472 1% of normal Chs2 enzyme activity (Nagahashi et al., 1995). The *Kkv-mos::NG* protein differs from
473 *Kkv::NG* by a series of mutations that lead to 8 amino acid changes (in the CS-C domain (pfam 03142))
474 that are found in several mosquito species (e.g *Aedes aegypti*, *Aedes albopictus*, *Anopheles gambiae* str.
475 PEST, *Culex pipiens pallens*, *Anopheles quadrimaculatus*, *Anopheles sinensis*). In *Kkv-mos::NG* the

476 sequence from aa 702-909 is identical to the mosquito Chitin Synthase 1 proteins. The CS-C domain is
477 from aa 722 to aa 904 in *kkv* and is slightly larger than a region of ScCHS2 that was shown to contain
478 chitin synthase catalytic activity. The *UAS-kkv-mos-NG* plasmid (Addgene - 138958) was constructed
479 from *UAS-kkv::NG* by synthesis of the relevant region and by it being placed into *kkv-NG* by Gibson
480 assembly (this and several other DNA manipulations were done by EpochLifeSciences). The nucleic acid
481 sequence of *kkv-mos::NG* is provided in sequence file S5 and the protein sequence in S6.

482 **The HDR repair constructs**

483 The upstream, middle and downstream repair regions were synthesized by assembly of oligonucleotides
484 by EpochLifeSciences. The segments that comprised Neon Green and smGFP-HA were obtained by PCR
485 from plasmids obtained from Allelebiotech and Addgene (#63166) respectively, added in the correct
486 position by Gibson Assembly. The synthesized segment included several silent mutations to prevent re-
487 cutting by Crispr/Cas9. The repair segments were subcloned into pHD-DsRed vector (Addgene plasmid
488 #51434) resulting in pHD-DsRed-*kkv*-3 (Addgene – 138960 for the NG repair construct). The sequences
489 of the plasmids that contain the HDR repair constructs are provided in files S7 and S8. The sequences of
490 the *Kkv* proteins encoded by the two edited genes are provided in File S9 and S10. The construction of
491 the edited genes resulted in a two amino acid linker (AG) between the C terminal aa of *kkv* and the first
492 amino acid of NG (or smFP). A carton showing the strategy is provided in Fig 1.

493 **gRNA constructs:** Two plasmids that express the needed gRNAs were made by inserting
494 oligonucleotides (files S11) into the pCFD3-dU6:gRNA plasmid where they would be expressed from the
495 pU6-3 promoter (Addgene plasmid – 45946). These two plasmids are pCFD-pUG-DH1 (Addgene
496 138963) and pCFD-dUG-DO1 (Addgene - 138962).

497 **Transgenic Lines:** Injections of DNA into embryos were done by Rainbow Transgenics. The UAS
498 transgenes were injected into embryos that contained the VK00033 attP landing site (cytol location
499 65B2; 3L:6,442,676..6,442,676). The transgenes were marked by a *w⁺* gene and Go flies were crossed
500 to *w¹¹¹⁸*; TM3/TM2 flies and the progeny screened for eye color. G1 male flies with eye color were
501 crossed to *w*; TM3/TM6 female flies and stocks were established by crossing siblings.

502 The HDR construct and the gRNA constructs were both injected into *nos-Cas9* expressing embryos
503 (injections by RainbowTransgenics). The Go flies were crossed to *w*; TM3/TM2 flies and the G1 flies
504 were screened for candidate edits by the expression of DsRed. Numerous putative edits were obtained
505 by screening for RFP expression from the Phd-Ds-red vector used for HDR. Putative edit containing flies
506 were crossed to *w*; TM2/TM3 flies and stocks established by crossing siblings that contained the TM3
507 balancer. The Ds-Red expression was monitored and proved to be useful in later stock constructions.
508 We also generated fly stocks where the DsRed was removed by crossing edited male flies to *hs-cre*;
509 *TM3/TM2* females and then crossing *hs-cre*; *kkv::NG + DS-Red/TM3* males to *w*; *TM3/TM2* females. The
510 progeny from this cross were screened for *TM3* (and non-*TM2*) flies that did not express Ds-Red. Stocks
511 were established from such single male flies and characterized by PCR to insure they carried the edited
512 *Kkv-NG* gene but lacked Ds-red sequences. No phenotypic differences were observed between edited
513 flies that carried or did not carry Ds-Red. The presence of Ds-Red expression was convenient for

514 following the edited gene in crosses and it was used for some experiments where we were not imaging
515 an alternative red fluorescent protein or stain.

516 **Characterization of *kkv* edits.** Six independent lines were established for both types of edits. DNA was
517 isolated from these and assayed for the correct DNA changes by PCR followed by sequencing (the oligos
518 used for these experiments are in Table S1). Most of the lines appeared to be as designed and resulted
519 in the in frame fusion of the C terminus of Kkv and the fluorescent protein with the designed two amino
520 acid linker. Three *kkv-NG* and two *kkv-smGFP-HA* lines were retained and further characterized. No
521 differences were seen between the 3 NG edits and between the 2 smGFP edits. One line of each was
522 chosen as the standard for routine use. Both of these are available at the Bloomington Drosophila stock
523 center.

524 **Confocal Microscopy**

525 Immunostaining of fixed pupal epidermal cells during the deposition of cuticle is complicated by the
526 inability of the antibodies to penetrate cuticle after the early stages of its development. Thus, most of
527 the imaging experiments we carried out on Kkv in pupae were done by in vivo imaging of Kkv::NG. In a
528 small number of experiments we examined Kkv-NG in fixed tissue. In some we simply used the inherent
529 fluorescence of the neon green tag (sometimes combined with phalloidin staining of actin). In others we
530 used anti-NG immunostaining. Such tissue was only weakly fixed and we did not use animals that were
531 older than around 48 hr after white prepupae (awp). Otherwise, immunostaining of pupal and larval
532 tissues were done as described previously (Nagaraj and Adler, 2012). Imaging of live Kkv::NG containing
533 pupae was done on a Zeiss 780 confocal microscope in the Keck Center for Cellular Imaging. Stained
534 samples were examined on the same microscope.

535

536 **Comparison of *kkv::NG* and *kkv::smFP***

537 We estimated the brightness difference between the products of the *kkv::NG* and *kkv::smFP* edited
538 genes by live imaging both in the same confocal session using the same microscope conditions. We
539 measured the brightness of maximal projections of both types of animals and then subtracted the
540 background brightness. The ratio of brightness for *kkv::NG* and *kkv::smFP* was 14.7. To estimate the
541 relative amount of the two proteins present we needed to correct for the relative brightness of the two
542 fluorescent protein tags. We were unable to find a value for the brightness of *smFP* but we were able to
543 find a value for the progenitor of smFP, superfolder GFP and Neon-Green (Lambert and Thorn, 2019).
544 The relative brightness was 1.7, which gave an estimate that Kkv::NG was present in 8.65 fold higher
545 concentration than Kkv::smFP. Assuming Kkv::smFP has the same specific activity as wild type Kkv we
546 estimate the *kkv::smFP* cells only contain about 11% of the normal Kkv enzyme activity.

547

548 **Kkv topology experiments**

549 We obtained predictions for the number and locations of transmembrane domains from the following
550 programs: TMHMM2.0, TMPRED, Uniprot, PHDhtm and CCTOP. The CCTOP site returned predictions for
551 HMMTOP, Memsat, Octopus, Philius, Phobius, Pro, Prodiv, Scampi, ScampiMsa as well as CCTOP. 14
552 putative transmembrane domains were predicted by 13 or 14 of these 14 programs. These “consensus
553 sites are shown in Fig 6 and the specific TMHMM2.0 predictions are provided in Table S2. The specific
554 amino acids predicted to be in each transmembrane domain were often shifted by a few amino acids by
555 different programs but the putative transmembrane domains substantially overlapped.

556 To examine the topology of Kkv we drove the expression of *UAS-kkv-OH* or *UAS-kkv::NG* by *ptc-GAL4*.
557 This results in a stripe of expression along the anterior/posterior compartment boundary in wing discs.
558 Wing discs were dissected in PBS and fixed in the cold for 15'. The discs were then manually cut or
559 punctured to ensure the apical surface of the epithelial cells was exposed to antibody. They were then
560 incubated for 30' in PBS supplemented with 10% Sheep Serum. The discs were then stained overnight at
561 4°C in PBS, 10% sheep serum plus the desired antibody. The discs were then rinsed 4 times in PBS and
562 then stained with secondary antibody for 3 hrs at room temperature in PBS, 10% sheep serum plus
563 secondary antibody. After 4 rinses in PBS the discs were washed with PBST (PBS plus .3% triton X100)
564 followed by three additional washes in PBS. Finally the discs were mounted in ProLong Diamond. As a
565 control several of the fixed and cut discs had PBST substituted for PBS in all steps in the experiment. The
566 wing discs were examined on a Zeiss Axioskop II and photographed on a Spot Digital Camera (National
567 Diagnostics).

568

569 **Figure Legends**

570 Figure 1. A. Models for chitin deposition and Chitin Synthase. B. Cartoons showing the proteins
571 encoded by both UAS transgenes and edited genes. The asterisks indicates the R896K mutation. C. The
572 approach used for the editing of *kkv*. The upward arrows indicate the target locations of the two guide
573 RNAs. The upper part of the panel shows the 3' end of *kkv*.

574 Figure 2. The rescue of the wing phenotype of *kkv::smFP* by the expression of a UAS transgene driven by
575 *ap-Gal4*. A small region from the dorsal and ventral surface of the wing is shown for all genotypes. This
576 region is from the posterior region. Note the thin bent hairs on both surfaces of the *kkv::smFP*
577 homozygotes (EF) compared to those in wild type (AB) and *ap>kkv::NG* (CD) wings. Note the rescue in
578 the dorsal surface of *ap>kkv::NG; kkv::smFP/Df* wings (GH). This is due to *ap* only driving expression of
579 UAS transgenes in the dorsal surface cells. Note the failure to see rescue in *ap>kkv R896K::NG;*
580 *kkv::smFP* wings (IJ) establishing that only the expression of a functional Kkv protein provides rescue.
581 The rescue with *ap>kkv mos::NG* can be seen in the image of the dorsal surface of such wings (K)
582 compared to the ventral surface (L).

583 Figure 3. Localization of Kkv in the pupal wing. A-F. In vivo images of *kkv::NG* pupal wings. All except B
584 are shown with the same microscope settings. Note the clear labeling of the hairs in wings from 42-58
585 hr. In the oldest wings the hairs are fainter and the image is from the focal plane where the pedestals
586 are obvious. We did not detect hair labeling in the youngest wings (A) unless the image was enhance by

587 brightening in ImageJ or Photoshop (B). G,H,I. Shown is a *ap-Gal4/+; UAS-kkv::NG* pupal 36 hr wing
588 fixed and F-actin stained with phalloidin (red). Note the NeonGreen is external to the F-actin. One can
589 also see that the NeonGreen signal is in the hair membrane and does not extend to the center of the
590 hair. J,K,L. A fixed 48 hr *ap-Gal4/+; UAS-kkv::NG* wing stained for both NeonGreen (J-green) and F-actin
591 (L-phalloidin - red). Note the bright disc of F-actin staining at the base of the hair is not associated with
592 an accumulation of Kkv::NG.

593 Figure 4. Localization of Kkv. A. A low magnification image of a *kkv::NG* notum. B. A higher
594 magnification image of part of a *kkv::NG* notum. Note the stripes of Kkv::NG along the proximal distal
595 axis of the bristles. C (C' and C''). A high magnification image of a bristle from a *UAS-ChtVis/+; neur-*
596 *Gal4/ kkv::NG/+* bristle. Note the relatively smooth bands of chitin (red) and the punctate stripes of
597 Kkv::NG (green) and the association between the two. D,E,F. Two bristles from a *neur-Gal4/kkv::NG*
598 pupae immunostained for NeonGreen (green-D) and Kkv (red-F). E is the merged image and shows the
599 high degree of co-immunostaining. G,H,I. Bristles from a *neur-Gal4/kkv-OH* pupae immunostained for
600 ollas (green-G) and Kkv (red-I). H is the merged image and shows the high degree of co-
601 immunostaining. J,K,L. Pupal wings from *ap-Gal4/+; UAS-kkv::NG* immunostained for NeonGreen
602 (green-J) and Kkv (red-L). K is the merged imaged and shows a high degree of co-localization.

603 Figure 5. Factors that mediate the localization of Kkv in stripes in bristles. A. A *sn f; kkv::NG* bristle by in
604 vivo imaging. The lack of the large F-actin bundles due to the loss of *sn* and *f* leads to highly abnormal
605 shape and abnormal patterning of Kkv::NG stripes. B. A *sn f; UAS-ChtVis/+; neur-Gal4/+* bristle by in vivo
606 imaging. The lack of the large F-actin bundles due to the loss of *sn* and *f* leads to highly abnormal bristle
607 shape and to abnormal patterning of chitin. C,D,E. A *sn f; UAS-ChtVis/+; neur-Gal4 kkv::NG/kkv::NG*
608 bristle by in vivo imaging. The lack of the large F-actin bundles due to the loss of *sn* and *f* leads to highly
609 abnormal shape and abnormal patterning of both chitin (C - red) and Kkv::NG (E - green) stripes. Note
610 the close association of Kkv and chitin (D- merged image, arrow) even though the pattern as a whole is
611 highly abnormal. F. A *UAS-dyl RNAi; neur-Gal4 kkv::NG/kkv::NG* thorax by in vivo imaging. Note the
612 bulged bristle (arrow) and the lack/great reduction of Kkv stripes. G A *UAS-Rab11-RNAi; neur-Gal4*
613 *kkv::NG/kkv::NG* bristle by in vivo imaging. Note the stub bristle phenotype (arrow) and the lack of
614 Kkv::NG stripes. H,I,J. A *UAS-Ruby-Lifeact; neur-Gal4 kkv::NG/kkv::NG* bristle showing the large bundles
615 of F-actin (H - red) and stripes of Kkv::NG (J - green). H', I', L' are higher magnification images where the
616 overlap between the F-actin bundles and Kkv::NG stripes is obvious. KLM. *Kkv::NG* bristles
617 immunostained with anti-Dyl antibody (K - red) and anti-NeonGreen antibody (M - green). In the
618 merged image (L) the interdigitated stripes of red and green can be seen (arrow).

619 Figure 6. Orthogonal cross sections of bristles of various genotypes. A. *kkv::NG* shows a distinct pattern
620 of stripes. B. *UAS-ChtVis/+; neur-Gal4 kkv::NG/kkv::NG* shows the close association of the chitin bands
621 and the stripes of Kkv::NG. In many cases the chitin is external to Kkv::NG (arrows). C. *UAS-Rab11-RNAi;*
622 *neur-Gal4 kkv::NG/kkv::NG* bristles show a failure in the localization of Kkv to the plasma membrane. D.
623 *UAS-dyl RNAi; neur-Gal4 kkv::NG/kkv::NG* bristles show much of the Kkv::NG is inserted into the plasma
624 membrane but it is not localized into the strip pattern (e.g. A). E. *sn f; kkv::NG* bristles have an abnormal
625 cross section and evidence for abnormal stripes of Kkv::NG are evident (arrows). F. *sn f; UAS-ChtVis;*
626 *neur-Gal4 kkv::NG/kkv::NG* bristles show the expected abnormal cross section shape with the irregular

627 banding of Kkv::NG and chitin. Note the close association of Kkv::NG and chitin (arrows) even in these
628 very abnormal bristles.

629 Fig 7. Topology of Kkv. A. *ptc-Gal4 UAS-kkv::NG* (or *UAS-kkv-OH*) wing discs where *kkv* is expressed in a
630 stripe immunostained with various antibodies with or without detergent treatment (PBST vs PBS). B. A
631 cartoon showing the consensus transmembrane domains as described in the Methods. The location of
632 the epitope recognized by each of the antibodies. The data indicate that the amino terminus is
633 cytoplasmic and the carboxy terminus is extracellular.

634 Acknowledgements

635 This research was supported by funds provided by the W. R. Kenan Chair to the author and limited
636 personal funds of the author. The author thanks H.S. Tzu for helpful conversations. “We acquired
637 confocal images using the Keck Center Zeiss 780 Confocal microscopy system (NIH OD016446). We
638 acquired Scanning Electron Microscope images at the Advanced Microscopy Facility at the University of
639 Virginia. The images were obtained on a Zeiss VP HD SEM field purchased with a grant from the NIH
640 (NIH 1S10OD011966). The author is retiring and closing his laboratory in May 2020. Hence, any
641 requests for reagents or additional information should be made prior to then.

642

643 References

- 644 **Adler, P. N.** (2017). Gene expression and morphogenesis during the deposition of *Drosophila* wing
645 cuticle. *Fly (Austin)* **11**, 194-199.
- 646 **Adler, P. N., Sobala, L. F., Thom, D. and Nagaraj, R.** (2013). *dusky-like* is required to maintain the
647 integrity and planar cell polarity of hairs during the development of the *Drosophila* wing.
648 *Developmental biology* **379**, 76-91.
- 649 **Bischof, J., Maeda, R. K., Hediger, M., Karch, F. and Basler, K.** (2007). An optimized transgenesis system
650 for *Drosophila* using germ-line-specific phiC31 integrases. *Proceedings of the National Academy*
651 *of Sciences of the United States of America* **104**, 3312-3317.
- 652 **Bouligand, Y.** (1972). Twisted fibrous arrangements in biological materials and cholesteric mesophases.
653 *Tissue Cell* **4**, 189-217.
- 654 **Broehan, G., Zimoch, L., Wessels, A., Ertas, B. and Merzendorfer, H.** (2007). A chymotrypsin-like serine
655 protease interacts with the chitin synthase from the midgut of the tobacco hornworm. *J Exp Biol*
656 **210**, 3636-3643.
- 657 **Cabib, E. and Bowers, B.** (1971). Chitin and yeast budding. Localization of chitin in yeast bud scars. *J Biol*
658 *Chem* **246**, 152-159.
- 659 **Calero-Cuenca, F. J. and Sotillos, S.** (2018). Nuf and Rip11 requirement for polarity determinant
660 recycling during *Drosophila* development. *Small GTPases* **9**, 352-359.
- 661 **Chanut-Delalande, H., Ferrer, P., Payre, F. and Plaza, S.** (2012). Effectors of tridimensional cell
662 morphogenesis and their evolution. *Seminars in cell & developmental biology* **23**, 341-349.
- 663 **Chaudhari, S. S., Arakane, Y., Specht, C. A., Moussian, B., Boyle, D. L., Park, Y., Kramer, K. J., Beman,**
664 **R. W. and Muthukrishnan, S.** (2011). Knickkopf protein protects and organizes chitin in the
665 newly synthesized insect exoskeleton. *Proceedings of the National Academy of Sciences of the*
666 *United States of America* **108**, 17028-17033.

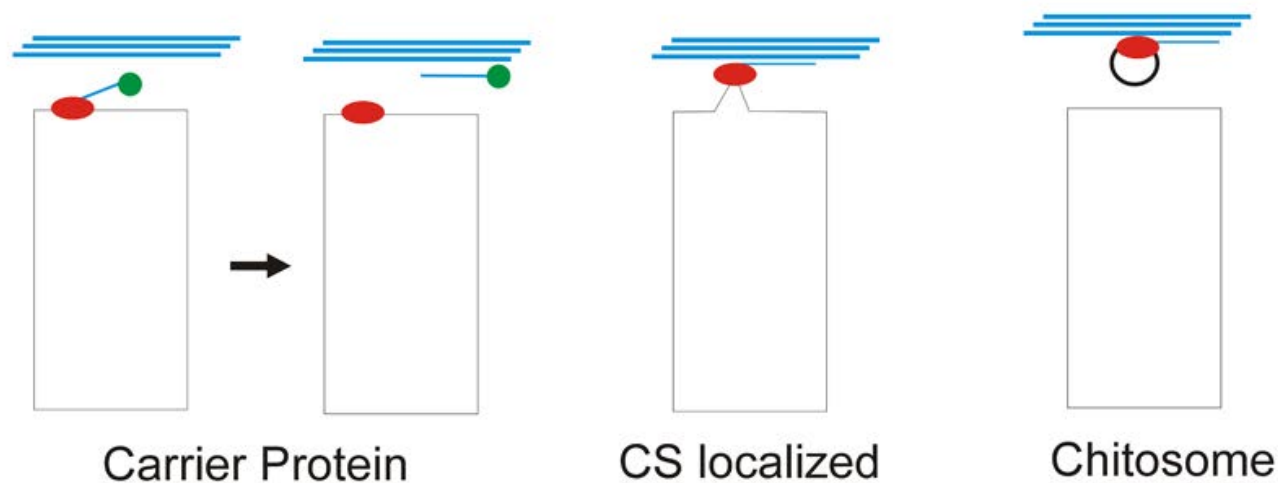
- 667 **Chuang, J. S. and Schekman, R. W.** (1996). Differential trafficking and timed localization of two chitin
668 synthase proteins, Chs2p and Chs3p. *J Cell Biol* **135**, 597-610.
- 669 **Devine, W. P., Lubarsky, B., Shaw, K., Luschnig, S., Messina, L. and Krasnow, M. A.** (2005). Requirement
670 for chitin biosynthesis in epithelial tube morphogenesis. *Proceedings of the National Academy of*
671 *Sciences of the United States of America* **102**, 17014-17019.
- 672 **Dietzl, G., Chen, D., Schnorrer, F., Su, K. C., Barinova, Y., Fellner, M., Gasser, B., Kinsey, K., Oettel, S.,**
673 **Scheiblaue, S., et al.** (2007). A genome-wide transgenic RNAi library for conditional gene
674 inactivation in *Drosophila*. *Nature* **448**, 151-156.
- 675 **Dorfmueller, H. C., Ferenbach, A. T., Borodkin, V. S. and van Aalten, D. M.** (2014). A structural and
676 biochemical model of processive chitin synthesis. *J Biol Chem* **289**, 23020-23028.
- 677 **Elieh-Ali-Komi, D. and Hamblin, M. R.** (2016). Chitin and Chitosan: Production and Application of
678 Versatile Biomedical Nanomaterials. *Int J Adv Res (Indore)* **4**, 411-427.
- 679 **Fernandes, I., Chanut-Delalande, H., Ferrer, P., Latapie, Y., Waltzer, L., Affolter, M., Payre, F. and Plaza,**
680 **S.** (2010). Zona pellucida domain proteins remodel the apical compartment for localized cell
681 shape changes. *Dev Cell* **18**, 64-76.
- 682 **Foltman, M., Filali-Mouneef, Y., Crespo, D. and Sanchez-Diaz, A.** (2018). Cell polarity protein Spa2
683 coordinates Chs2 incorporation at the division site in budding yeast. *PLoS genetics* **14**,
684 e1007299.
- 685 **Gohlke, S., Muthukrishnan, S. and Merzendorfer, H.** (2017). In Vitro and In Vivo Studies on the
686 Structural Organization of Chs3 from *Saccharomyces cerevisiae*. *Int J Mol Sci* **18**.
- 687 **Guild, G. M., Connolly, P. S., Vranich, K. A., Shaw, M. K. and Tilney, L. G.** (2002). Actin filament turnover
688 removes bundles from *Drosophila* bristle cells. *Journal of cell science* **115**, 641-653.
- 689 **Hatan, M., Shinder, V., Israeli, D., Schnorrer, F. and Volk, T.** (2011). The *Drosophila* blood brain barrier
690 is maintained by GPCR-dependent dynamic actin structures. *J Cell Biol* **192**, 307-319.
- 691 **Hernandez-Gonzalez, M., Bravo-Plaza, I., Pinar, M., de Los Rios, V., Arst, H. N., Jr. and Penalva, M. A.**
692 (2018). Endocytic recycling via the TGN underlies the polarized hyphal mode of life. *PLoS*
693 *genetics* **14**, e1007291.
- 694 **Jovine, L., Darie, C. C., Litscher, E. S. and Wassarman, P. M.** (2005). Zona pellucida domain proteins.
695 *Annual review of biochemistry* **74**, 83-114.
- 696 **Jovine, L., Qi, H., Williams, Z., Litscher, E. and Wassarman, P. M.** (2002). The ZP domain is a conserved
697 module for polymerization of extracellular proteins. *Nature cell biology* **4**, 457-461.
- 698 **Karouzou, M. V., Spyropoulos, Y., Iconomidou, V. A., Cornman, R. S., Hamodrakas, S. J. and Willis, J. H.**
699 (2007). *Drosophila* cuticular proteins with the R&R Consensus: annotation and classification with
700 a new tool for discriminating RR-1 and RR-2 sequences. *Insect biochemistry and molecular*
701 *biology* **37**, 754-760.
- 702 **Knafler, H. C., Smaczynska-de, R., II, Walker, L. A., Lee, K. K., Gow, N. A. R. and Ayscough, K. R.** (2019).
703 AP-2-Dependent Endocytic Recycling of the Chitin Synthase Chs3 Regulates Polarized Growth in
704 *Candida albicans*. *MBio* **10**.
- 705 **Kozubowski, L., Panek, H., Rosenthal, A., Bloecher, A., DeMarini, D. J. and Tatchell, K.** (2003). A Bni4-
706 Glc7 phosphatase complex that recruits chitin synthase to the site of bud emergence. *Mol Biol*
707 *Cell* **14**, 26-39.
- 708 **Lambert, T. and Thorn, K.** (2019). FPbase.org - The Fluorescent Protein Database.
- 709 **Latge, J. P., Mouyna, I., Tekaia, F., Beauvais, A., Debeaupuis, J. P. and Nierman, W.** (2005). Specific
710 molecular features in the organization and biosynthesis of the cell wall of *Aspergillus fumigatus*.
711 *Med Mycol* **43 Suppl 1**, S15-22.
- 712 **Leal-Morales, C. A., Bracker, C. E. and Bartnicki-Garcia, S.** (1994). Subcellular localization, abundance
713 and stability of chitin synthetases 1 and 2 from *Saccharomyces cerevisiae*. *Microbiology* **140 (Pt**
714 **9)**, 2207-2216.

- 715 **Maue, L., Meissner, D. and Merzendorfer, H.** (2009). Purification of an active, oligomeric chitin synthase
716 complex from the midgut of the tobacco hornworm. *Insect biochemistry and molecular biology*
717 **39**, 654-659.
- 718 **McGuire, S. E., Mao, Z. and Davis, R. L.** (2004). Spatiotemporal gene expression targeting with the
719 TARGET and gene-switch systems in Drosophila. *Sci STKE* **2004**, pl6.
- 720 **Merzendorfer, H.** (2006). Insect chitin synthases: a review. *J Comp Physiol B* **176**, 1-15.
721 ---- (2011). The cellular basis of chitin synthesis in fungi and insects: common principles and differences.
722 *European journal of cell biology* **90**, 759-769.
- 723 **Merzendorfer, H. and Zimoch, L.** (2003). Chitin metabolism in insects: structure, function and regulation
724 of chitin synthases and chitinases. *J Exp Biol* **206**, 4393-4412.
- 725 **Mitchell, H. K., Edens, J. and Petersen, N. S.** (1990). Stages of cell hair construction in Drosophila.
726 *Developmental genetics* **11**, 133-140.
- 727 **Moussian, B.** (2013). The apical plasma membrane of chitin-synthesizing epithelia. *Insect science* **20**,
728 139-146.
- 729 **Moussian, B., Letizia, A., Martinez-Corrales, G., Rotstein, B., Casali, A. and Llimargas, M.** (2015).
730 Deciphering the genetic programme triggering timely and spatially-regulated chitin deposition.
731 *PLoS genetics* **11**, e1004939.
- 732 **Moussian, B., Schwarz, H., Bartoszewski, S. and Nusslein-Volhard, C.** (2005). Involvement of chitin in
733 exoskeleton morphogenesis in Drosophila melanogaster. *Journal of morphology* **264**, 117-130.
- 734 **Moussian, B., Seifarth, C., Muller, U., Berger, J. and Schwarz, H.** (2006a). Cuticle differentiation during
735 Drosophila embryogenesis. *Arthropod structure & development* **35**, 137-152.
- 736 **Moussian, B., Tang, E., Tønning, A., Helms, S., Schwarz, H., Nusslein-Volhard, C. and Uv, A. E.** (2006b).
737 Drosophila Knickkopf and Retroactive are needed for epithelial tube growth and cuticle
738 differentiation through their specific requirement for chitin filament organization. *Development*
739 **133**, 163-171.
- 740 **Moussian, B., Veerkamp, J., Muller, U. and Schwarz, H.** (2007). Assembly of the Drosophila larval
741 exoskeleton requires controlled secretion and shaping of the apical plasma membrane. *Matrix*
742 *biology : journal of the International Society for Matrix Biology* **26**, 337-347.
- 743 **Muszkiet, L., Aïmanianda, V., Mellado, E., Gribaldo, S., Alcazar-Fuoli, L., Szweczyk, E., Prevost, M. C.**
744 **and Latge, J. P.** (2014). Deciphering the role of the chitin synthase families 1 and 2 in the in vivo
745 and in vitro growth of *Aspergillus fumigatus* by multiple gene targeting deletion. *Cell Microbiol*
746 **16**, 1784-1805.
- 747 **Nagahashi, S., Sudoh, M., Ono, N., Sawada, R., Yamaguchi, E., Uchida, Y., Mio, T., Takagi, M., Arisawa,**
748 **M. and Yamada-Okabe, H.** (1995). Characterization of chitin synthase 2 of *Saccharomyces*
749 *cerevisiae*. Implication of two highly conserved domains as possible catalytic sites. *J Biol Chem*
750 **270**, 13961-13967.
- 751 **Nagaraj, R. and Adler, P. N.** (2012). Dusky-like functions as a Rab11 effector for the deposition of cuticle
752 during Drosophila bristle development. *Development* **139**, 906-916.
- 753 **Ostrowski, S., Dierick, H. A. and Bejsovec, A.** (2002). Genetic control of cuticle formation during
754 embryonic development of Drosophila melanogaster. *Genetics* **161**, 171-182.
- 755 **Ozturk-Colak, A., Moussian, B., Araujo, S. J. and Casanova, J.** (2016). A feedback mechanism converts
756 individual cell features into a supracellular ECM structure in Drosophila trachea. *Elife* **5**.
- 757 **Park, S. H., Cheong, C., Idoyaga, J., Kim, J. Y., Choi, J. H., Do, Y., Lee, H., Jo, J. H., Oh, Y. S., Im, W., et al.**
758 (2008). Generation and application of new rat monoclonal antibodies against synthetic FLAG and
759 OLLAS tags for improved immunodetection. *J Immunol Methods* **331**, 27-38.
- 760 **Perkins, L. A., Holderbaum, L., Tao, R., Hu, Y., Sopko, R., McCall, K., Yang-Zhou, D., Flockhart, I., Binari,**
761 **R., Shim, H. S., et al.** (2015). The Transgenic RNAi Project at Harvard Medical School: Resources
762 and Validation. *Genetics* **201**, 843-852.

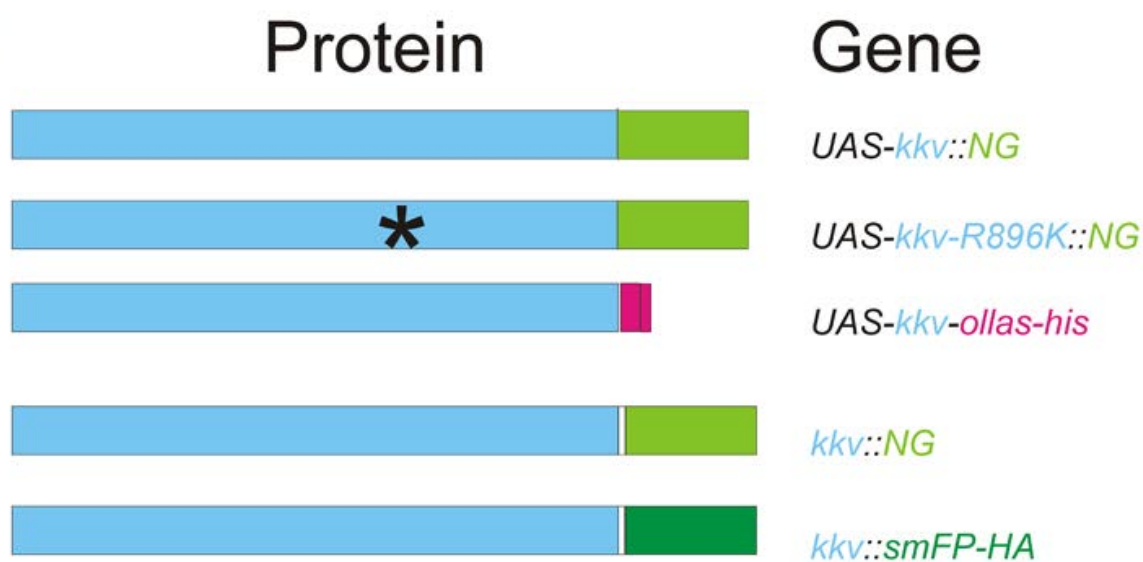
- 763 **Polko, J. K. and Kieber, J. J.** (2019). The Regulation of Cellulose Biosynthesis in Plants. *Plant Cell* **31**, 282-
764 296.
- 765 **Ren, N., Zhu, C., Lee, H. and Adler, P. N.** (2005). Gene expression during Drosophila wing morphogenesis
766 and differentiation. *Genetics* **171**, 625-638.
- 767 **Riedl, J., Crevenna, A. H., Kessenbrock, K., Yu, J. H., Neukirchen, D., Bista, M., Bradke, F., Jenne, D.,
768 Holak, T. A., Werb, Z., et al.** (2008). Lifeact: a versatile marker to visualize F-actin. *Nat Methods*
769 **5**, 605-607.
- 770 **Sacristan, C., Manzano-Lopez, J., Reyes, A., Spang, A., Muniz, M. and Roncero, C.** (2013).
771 Oligomerization of the chitin synthase Chs3 is monitored at the Golgi and affects its endocytic
772 recycling. *Mol Microbiol* **90**, 252-266.
- 773 **Saiz-Baggetto, S., Mendez, E., Quilis, I., Igual, J. C. and Bano, M. C.** (2017). Chimeric proteins tagged
774 with specific 3xHA cassettes may present instability and functional problems. *PLoS One* **12**,
775 e0183067.
- 776 **Santos, B. and Snyder, M.** (1997). Targeting of chitin synthase 3 to polarized growth sites in yeast
777 requires Chs5p and Myo2p. *J Cell Biol* **136**, 95-110.
- 778 **Shaner, N. C., Lambert, G. G., Chammas, A., Ni, Y., Cranfill, P. J., Baird, M. A., Sell, B. R., Allen, J. R.,
779 Day, R. N., Israelsson, M., et al.** (2013). A bright monomeric green fluorescent protein derived
780 from Branchiostoma lanceolatum. *Nat Methods* **10**, 407-409.
- 781 **Sobala, L. F. and Adler, P. N.** (2016). The Gene Expression Program for the Formation of Wing Cuticle in
782 Drosophila. *PLoS genetics* **12**, e1006100.
- 783 **Sobala, L. F., Wang, Y. and Adler, P. N.** (2015). ChtVis-Tomato, a genetic reporter for in vivo visualization
784 of chitin deposition in Drosophila. *Development* **142**, in press.
- 785 **Thurmond, J., Goodman, J. L., Strelets, V. B., Attrill, H., Gramates, L S., Marygold, S. J., Matthews, B.
786 B., Millburn, G., Antonazzo, G., Trovisco, V., et al.** (2018). FlyBase 2.0: the next generation.
787 *Nucleic acids research* **47**, D759-D765.
- 788 **Tilney, L. G., Connelly, P. S., Ruggiero, L., Vranich, K. A., Guild, G. M. and Derosier, D.** (2004). The role
789 actin filaments play in providing the characteristic curved form of Drosophila bristles. *Mol Biol*
790 *Cell* **15**, 5481-5491.
- 791 **Tilney, L. G., Tilney, M. S. and Guild, G. M.** (1995). F actin bundles in Drosophila bristles. I. Two filament
792 cross-links are involved in bundling. *J Cell Biol* **130**, 629-638.
- 793 **Tonning, A., Hemphala, J., Tang, E., Nannmark, U., Samakovlis, C. and Uv, A.** (2005). A transient luminal
794 chitinous matrix is required to model epithelial tube diameter in the Drosophila trachea. *Dev*
795 *Cell* **9**, 423-430.
- 796 **Turner, C. M. and Adler, P. N.** (1998). Distinct roles for the actin and microtubule cytoskeletons in the
797 morphogenesis of epidermal hairs during wing development in Drosophila. *Mech Dev* **70**, 181-
798 192.
- 799 **Viswanathan, S., Williams, M. E., Bloss, E. B., Stasevich, T. J., Speer, C. M., Nern, A., Pfeiffer, B. D.,
800 Hooks, B. M., Li, W. P., English, B. P., et al.** (2015). High-performance probes for light and
801 electron microscopy. *Nat Methods* **12**, 568-576.
- 802 **Welz, T., Wellbourne-Wood, J. and Kerkhoff, E.** (2014). Orchestration of cell surface proteins by Rab11.
803 *Trends Cell Biol* **24**, 407-415.
- 804 **Willis, J. H.** (2010). Structural cuticular proteins from arthropods: annotation, nomenclature, and
805 sequence characteristics in the genomics era. *Insect biochemistry and molecular biology* **40**, 189-
806 204.
- 807 **Wong, L. L. and Adler, P. N.** (1993). Tissue polarity genes of Drosophila regulate the subcellular location
808 for prehair initiation in pupal wing cells. *J Cell Biol* **123**, 209-221.

- 809 **Yabe, T., Yamada-Okabe, T., Nakajima, T., Sudoh, M., Arisawa, M. and Yamada-Okabe, H.** (1998).
810 Mutational analysis of chitin synthase 2 of *Saccharomyces cerevisiae*. Identification of additional
811 amino acid residues involved in its catalytic activity. *Eur J Biochem* **258**, 941-947.
- 812 **Zhang, X. and Zhu, K. Y.** (2013). Biochemical characterization of chitin synthase activity and inhibition in
813 the African malaria mosquito, *Anopheles gambiae*. *Insect science* **20**, 158-166.
- 814 **Zimoch, L. and Merzendorfer, H.** (2002). Immunolocalization of chitin synthase in the tobacco
815 hornworm. *Cell Tissue Res* **308**, 287-297.
816

A



B



C

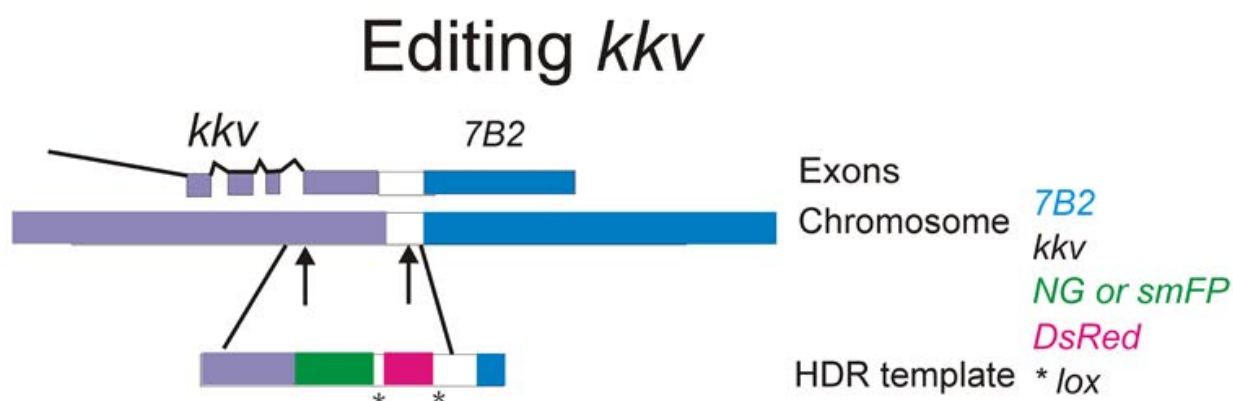


Figure 1

dorsal

ventral

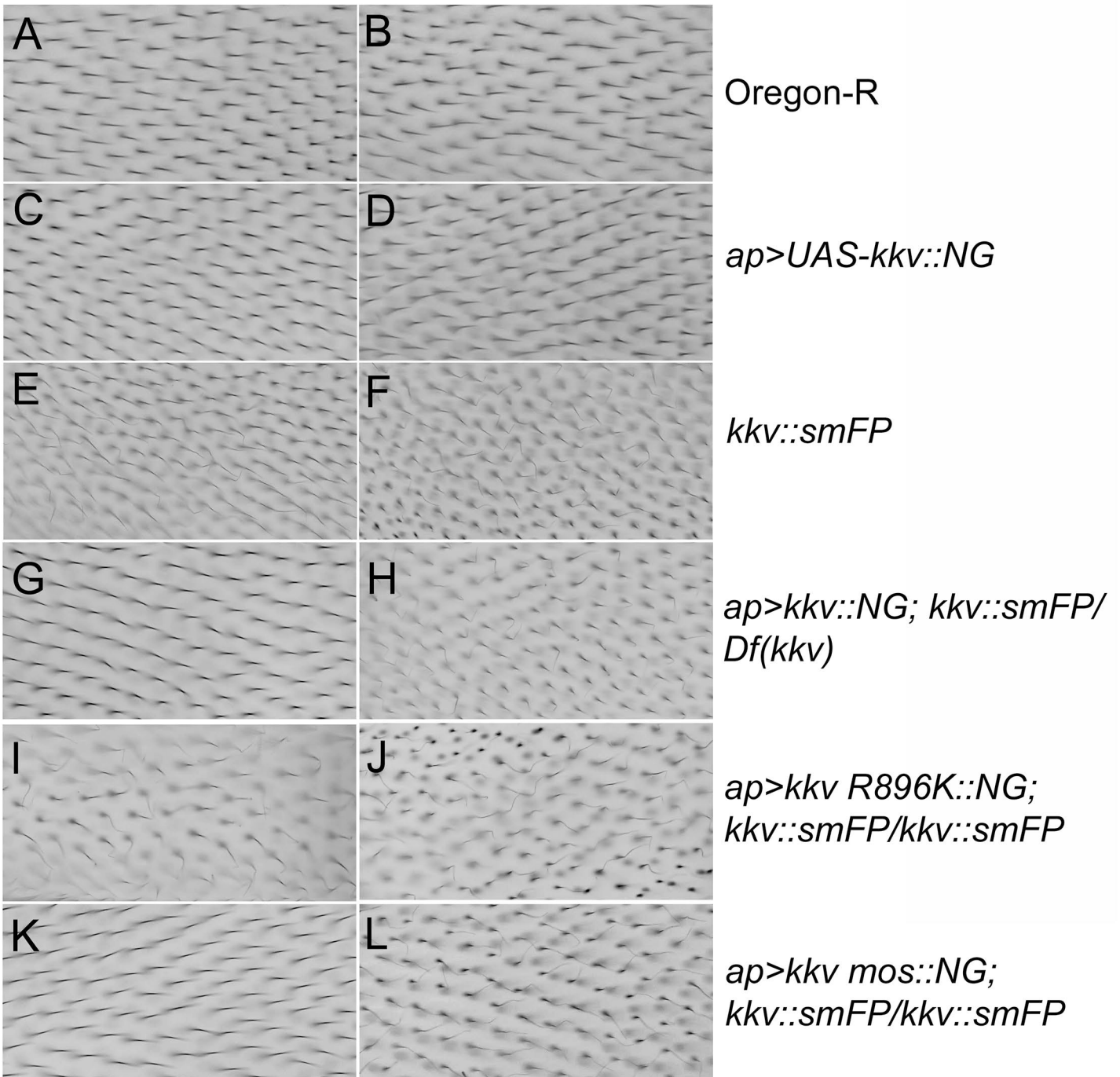


Fig 2

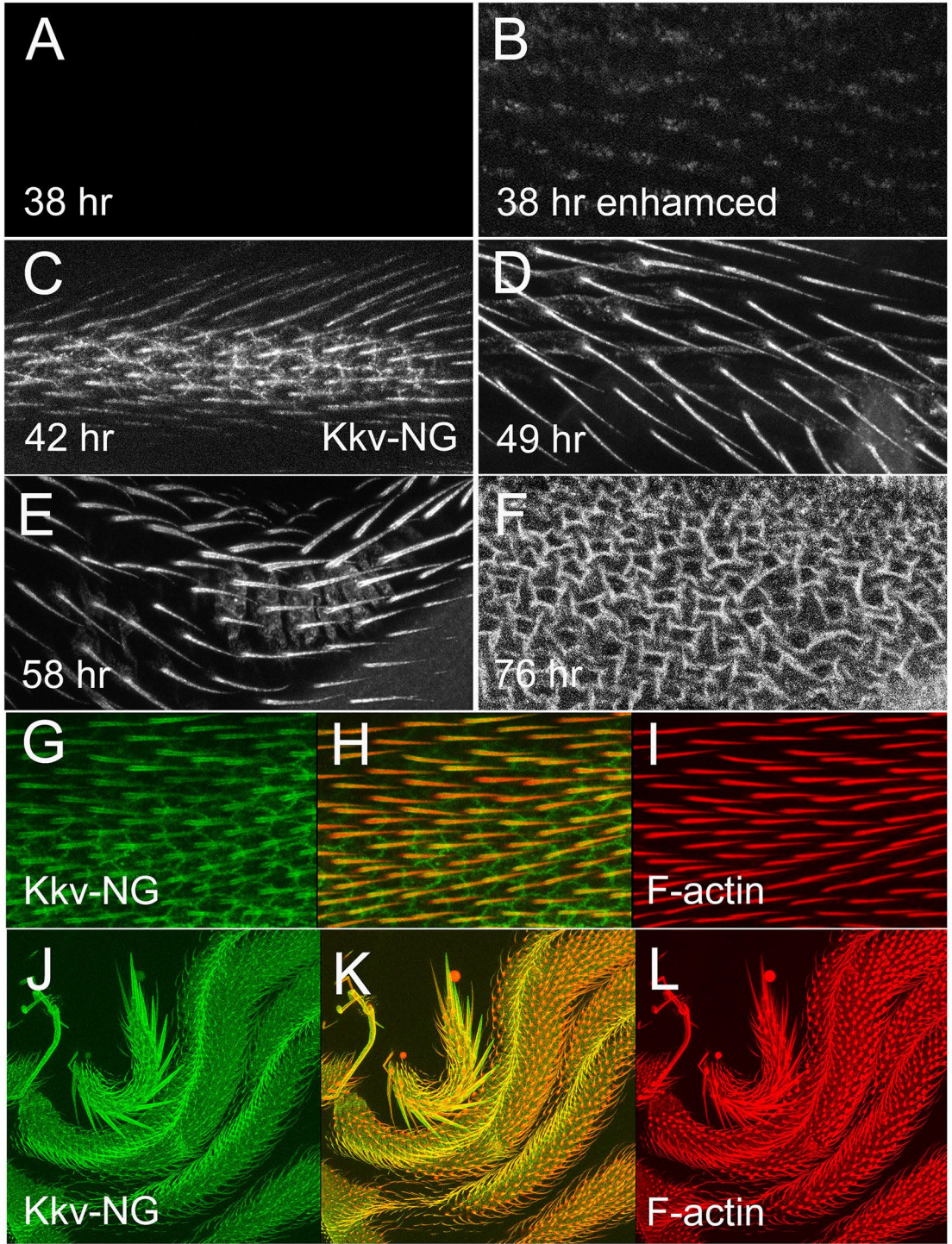


Figure 3

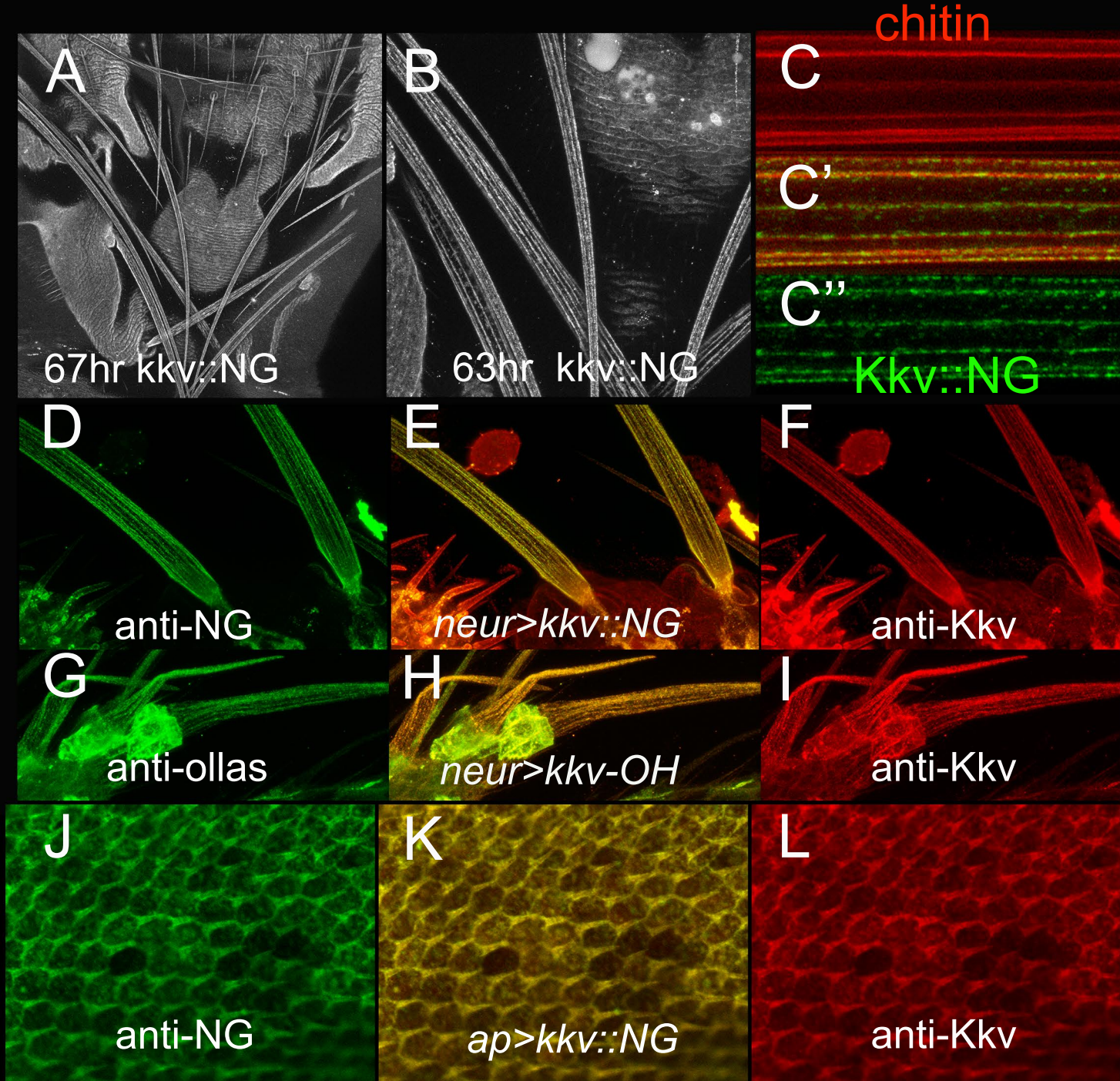


Figure 4

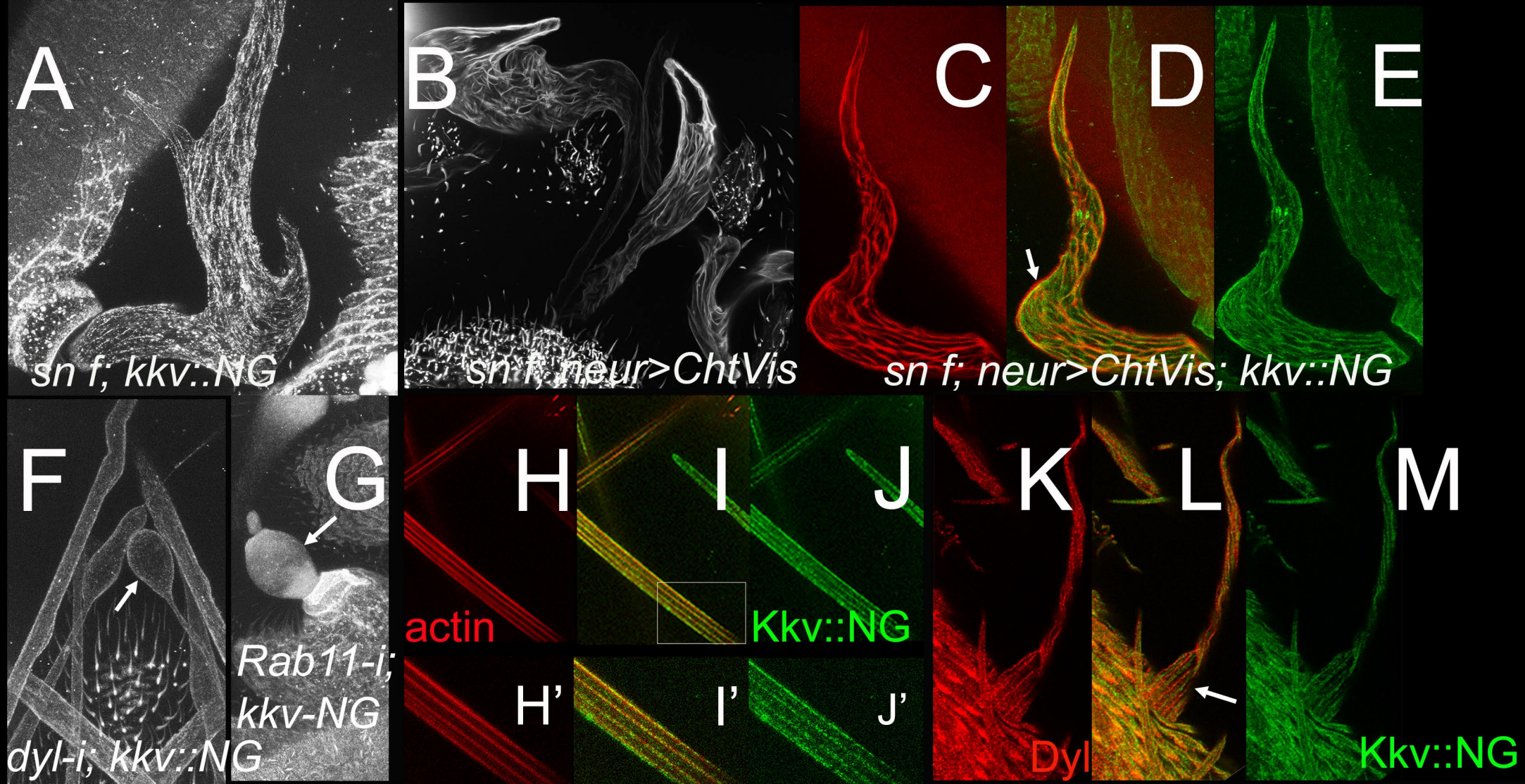


Fig 5

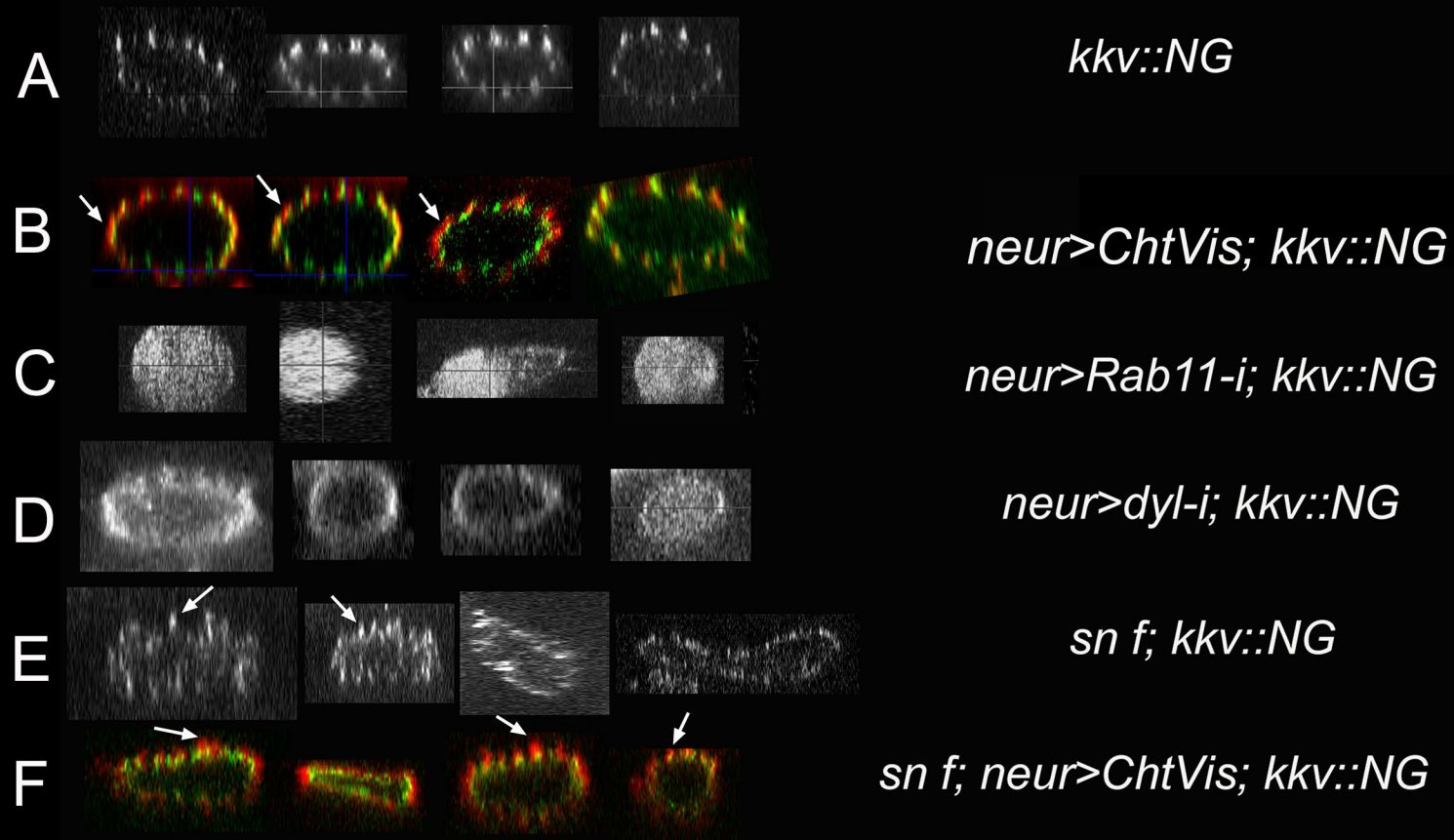


Figure 6

